Spatial Attention Weakly Modulates Visual Responses in the Lateral Geniculate Nucleus

Henry J. Alitto[1,2+] Jeffrey S. Johnson[1,2], and W. Martin Usrey[1,2]

[1] Center for Neuroscience, University of California, Davis, Davis, CA, 95618, USA
[2] Neurobiology, Physiology, and Behavior University of California, Davis, Davis, CA, 95618, USA
[+] hjalitto@ucdavis.edu

Running title: Spatial attention in the LGN

Author Contributions: HJA and WMU designed the research, HJA performed the research, HJA and JSJ analyzed data, HJA and WMU wrote the paper

Number of Figures: 10
Number of Tables: 0
Number of Mulitmedia: 0
Number of words for Abstract: 247
Number of words for Significance Statement: 92
Number of words for Introduction: 655
Number of words for Discussion: 1615

Acknowledgements: We thank K.E. Neverkovec, D.J. Sperka and R. Oates for expert technical assistance.

Conflict of Interest: Authors report no conflict of interest

Funding sources: This work was supported by NIH grants EY012576, EY036242, and P50MH132642

ABSTRACT

Visual responses in the cerebral cortex are strongly influenced by shifts in spatial attention. This modulation of visual processing includes changes in firing rate, decreased response variability, and decreased interneuronal correlations; all of which are thought to underlie enhanced visual perception near the center of attention at the cost of visual perception at other locations. Visual information from the retina is relayed to primary visual cortex via neurons in the lateral geniculate nucleus (LGN) of the dorsal thalamus. Although early studies describe an enhancement of LGN activity with spatial attention, more recent work has cast doubt on this view. Given its strategic position as the gateway to the cortex, an understanding of the effects of attention on visual processing in the LGN is important. We therefore performed experiments to reexamine the influence of covert spatial attention on the spiking activity of single units in the macaque LGN and applied a broad set of analyses and functional metrics to assess possible effects. Our results reveal a statistically significant effect of spatial attention in the LGN: firing rates were slightly higher and more reliable when monkeys directed attention towards the receptive fields of recorded neurons compared to when attention was directed to different retinotopic locations. However, effects were much smaller than previously reported (~1% vs ~4%) and further analyses suggest that effects are weak and inconsistent. Thus, while spatial attention does exert an influence in the LGN, its effects are weak and may have limited impact on downstream processing.

Significance Statement

The lateral geniculate nucleus (LGN) is a critical relay in the visual system, shaping the flow of sensory information from the eye to the brain. Although higher-order brain regions show strong modulation by attention, it remains unclear whether the LGN is similarly affected. By directly

recording LGN activity in monkeys performing a covert attention task, we found that spatial attention produces only weak and inconsistent modulation of visual responses. These findings suggest that the LGN largely operates independently of spatial attention, highlighting a potential boundary between early sensory processing and cognitive control.

Introduction

Spatial attention refers to the allocation of perceptual resources to enhance the processing of visual information at a specific spatial location, improving stimulus detectability and behavioral responsivity (Posner, 1980). While a full understanding of spatial attention is still emerging, the neural correlates of volitional spatial attention are generally believed to involve top-down processes (Maunsell, 2015; Boshra and Kastner, 2022; Martinez-Trujillo, 2022). These processes modulate fundamental aspects of visual responses in the cerebral cortex, including changes in firing rate, decreased response variability, and decreased neuronal correlations (Luck et al., 1997; McAdams and Reid, 2005; Cohen and Maunsell, 2009; Mitchell et al., 2009). Consistent with a top-down framework, the influence of spatial attention on visual response properties is greatest towards the top of the visual hierarchy (e.g., IT cortex) and weakest in primary visual cortex (V1), the initial stage of visual processing in the cortex (Luck et al., 1997; Kastner and Ungerleider, 2000; McAdams and Reid, 2005; Lauritzen et al., 2010; Ni and Maunsell, 2019; Meyyappan et al., 2025).

Along with the cortex, subcortical areas also play a role in spatial attention (Saalmann and Kastner, 2011; Zénon and Krauzlis, 2012; Zhou et al., 2016; Sherman and Usrey, 2021). Two of these areas, the superior colliculus in the midbrain and the pulvinar in the thalamus, receive strong, driving input from the cortex (Lynch et al., 1985; Sherman and Guillery, 2002; Cerkevich et al., 2014; Baldwin et al., 2017) and, thus, a route exists for cortical mechanisms to influence their response properties and communication with target structures. In contrast, neurons in the lateral geniculate nucleus (LGN) lack driving cortical input, instead receiving their driving input exclusively from the retina which is then relayed to cortex (reviewed in Usrey & Alitto, 2015) . Despite this, LGN activity has been reported to be influenced by spatial attention (O'Connor et al., 2002; McAlonan et al., 2008), potentially mediated by modulatory feedback pathways from the cortex and/or inhibitory circuits involving the thalamic reticular nucleus (TRN) (McAlonan et

al., 2008). The impact of attention on LGN activity remains unclear, though, as more recent work has not found effects of attention on visual processing in the LGN (Jiang et al., 2015; Shah et al., 2022).

Given the differences in past results and the importance of understanding the dynamics of visual signals delivered to cortex, we reexamined the influence of spatial attention on the spiking activity of LGN neurons in the macaque monkey and applied a broad set of analyses and functional metrics to assess possible effects. Moreover, recognizing that effects may be small, we collected data from a large sample of LGN neurons to strengthen the statistical analyses. Our results reveal small but significant effects of attention on the firing rate and reliability of LGN responses to visual stimuli. However, a deeper analysis of the data reveals that these effects are weak and inconsistent. Specifically, we found that shifting spatial attention towards LGN receptive fields was the equivalent of increasing the stimulus contrast by 1.25% or 1.0% for parvocellular and magnocellular neurons, respectively. Likewise, an ROC analysis indicates that an ideal observer would only be able to distinguish attend-toward trials from attend-away trials with 52% accuracy. Additionally, we did not observe a change in burst activity with shifts in spatial attention. Given that changes in burst firing are considered a reliable indicator of changes in thalamic network state (Sherman, 2001; McCormick et al., 2015), this is further evidence of the weak influence of spatial attention on LGN responses. Finally, by applying a linear classifier to pseudo-populations constructed from our recorded sample of LGN neurons, we found that attentional state could indeed be decoded at the population level. However, consistent with our single-cell analysis, this signal was largely driven by a small subset of neurons with stronger attentional modulation, rather than emerging from a distributed population code. Collectively, these results indicate that the modulation of LGN responses by spatial attention is statistically significant but functionally ineffectual.

MATERIALS AND METHODS

Two adult rhesus monkeys (Macaca mulatta; one male and one female) were used for electrophysiological recordings in this study. All experimental procedures conformed to the National Institutes of Health and the United States Department of Agriculture guidelines and were approved by the Institutional Animal Care and Use Committee at [**redacted for blind review**]. Under full surgical anesthesia, the animals received a cranial implant consisting of a head post for head stabilization and a recording cylinder that allowed access to the LGN.

Electrophysiological recordings. Extracellular recordings from the LGN were made with platinum-glass electrodes (1–2 MΩ; Alpha Omega) using a microdrive (40 mm electrode travel; Thomas Motorized Electrode Manipulator, Thomas Recording) mounted on the recording chamber. Online continuous voltage signals were amplified (A-M Systems), filtered (0.1–5 kHz), and recorded using a Micro1401 data acquisition system (28 kHz) and Spike2 software (Cambridge Electronic Design, CED). To extract action potentials, extracellular signals were high-pass filtered (stopband edge frequency = 500 Hz), thresholded, and clustered within the Spike2 software.

Visual Stimulation and Receptive Field Mapping. Visual stimuli were generated with a ViSaGe (Cambridge Research Systems) and presented on a gamma-corrected CRT monitor (Sony or Mitsubishi) positioned ~80 cm in front of the animal. The display had a resolution of 1024x768, a refresh rate of 100-140Hz, and a mean luminance of ~38 cd/m2. LGN receptive fields were manually mapped using small (<0.5°) user-controlled, computer-generated visual stimuli (custom software with Spike2 interface). The visual stimuli used for assessing spatial attention are described below.

Behavioral training and performance. Data was collected while the animals performed a spatial attention task (Figure 1A-B) while eye position and pupil size were monitored using an

Eye-Trac6 infrared eye tracker (Applied Science Laboratories) with a custom Spike2 interface. For this task, the animals initiated a trial by fixating a central fixation dot similar to the fixation dot used for passive fixation (hand mapping trials). The fixation dot was ~0.2° diameter, and the fixation window was 0.8°-1.2° diameter. After a short delay (0.5-1.0s), two sine wave gratings (temporal frequency = 5 Hz, spatial frequency = 1.0 cycles/°) appeared at equidistant locations from the fovea, typically at an eccentricity of 4-8°. During recording sessions, one stimulus was positioned inside the recorded LGN receptive field (dashed black circle; note: the dashed circle was not present in the actual stimulus display presented to the animals). Each sine wave grating was surrounded by a colored circle (one green, one red), and the color of the circles at each location was constant throughout the task. The color of the fixation dot (either red or green) indicated to the animal which grating was 90% likely to change contrast (valid trials) after a delay with an exponential hazard function of 0.6 – 1.8s. On 10% of the trials (invalid trials), the uncued grating increased in contrast (same hazard function). Because one stimulus was always inside the RF and the other outside, trials were further categorized based on the spatial relationship between the cued location and the RF. “Attend toward” trials (A) occurred when the cued stimulus—i.e., the one most likely to change contrast—was positioned inside the RF. “Attend away” trials (B) occurred when the cued stimulus was positioned outside the RF. This classification was used in all subsequent analyses to assess how spatial attention modulated LGN responses. The base contrast of the grating was set to be near the C50 (contrast to evoke a half-maximum response) of the recorded LGN neuron, as estimated through hand mapping. After the contrast change, the animal was given 1s to respond by making a saccade to the location of the change, and the animal was rewarded with a small juice reward. Psychophysical performance (accuracy and reaction time) for valid and invalid trials were compared to ensure that the animals were applying spatial attention as anticipated. Based on these comparisons, the contrast change was titrated so that the animal performed 20-30% better on cued trials relative to uncued trials.

164 **Analysis**

165 *Classification of neurons:* Based on the hand-mapping procedures described above, we
166 classified LGN neurons on two axes: cell-type and response polarity (Alitto et al., 2011). Cell
167 types were defined as magnocellular or parvocellular based on the C50 (C50 greater than 35%
168 were classified as parvocellular, C50 less than 35% were classified as magnocellular).
169 Response polarity (on-center cells vs off-center cells) was based on responses to increases and
170 decreases in luminance.

171 *Firing rate and spatial attention*: LGN neurons have linear responses to the presentation of
172 drifting sine wave gratings that are modulated by the phase of visual stimulus. To extract this
173 linear response, we calculated the average cycle histogram (cycle duration = 200 ms, bin size =
174 7.7 ms) for each trial and extracted the linear response as the F_1 from a Fourier transform with a
175 Hanning window (custom Matlab script). Based on the F_1 and F_0 (mean firing rate), the attention
176 index was defined as:

177 $$attention\ index = (FR_{toward} - FR_{away})/(FR_{toward} + FR_{away})$$

178 Here, the FR is the firing rate (either the F_0 or F_1) during attend toward and attend away trials.

179 *Equivalent Contrast Change:* Shifts in spatial attention are often analogized as being similar to
180 changes in stimulus contrast (Carrasco et al., 2004; Reynolds and Chelazzi, 2004). Given that
181 shifts in spatial attention cause changes in the firing rates of visual neurons, we wanted to
182 determine the changes in contrast that would have produced equivalent changes in firing rate.
183 In the current study, the baseline stimulus contrast was individually specified for each LGN
184 neuron, based on computer-aided hand mapping of the receptive field, to evoke 50% of the
185 cell's maximum response (C50). Since complete contrast response functions were not available
186 for the current data set, we created standardized parvocellular and magnocellular contrast
187 response functions from a separate sample of LGN neurons (Figure 3a; magnocellular: n = 33,

188 parvocellular: n = 87; 5-8 stimulus repeats per contrast) and applied the attentional changes in
189 firing onto this value to determine an effective/equivalent contrast change. For each recorded
190 neuron, we estimated the attention-driven change in firing rate as:

191 $$\Delta FR = \frac{FR_{toward} - FR_{away}}{FR_{toward}}$$

192 Using the standardized magnocellular and parvocellular contrast response functions, we then
193 estimated the contrast that would have evoked an equivalent response difference relative to the
194 C50. For example, if the attend-toward firing rate was 1.2x greater than the attend-away firing
195 rate, we would identify the contrast that would have evoked a response that was 1.2x the firing
196 rate evoked at C50. Based on this calculation we then defined attention equivalent contrast
197 change as:

198 $$\text{attention equivalent contrast change} = \frac{equivalent\ contrast - baseline\ contrast}{\text{baseline contrast}}$$

199 *ROC analysis of attentional modulation:* To further quantify the influence of spatial attention on
200 visual responses in the LGN, we performed an ROC analysis to determine how well an ideal
201 observer would be able to determine the focus of the animal's attention based solely on the trial-
202 by-trial distribution of F_1s across attend-toward and attend-away trials. Using the matlab function
203 perfcurve (bootstrap n = 1000), we determined if (a) attend toward trials were distinguishable
204 from spontaneous activity, (b) attend away trials were toward trials were distinguishable from
205 spontaneous activity, and (c) attend toward trials were distinguishable from attend away trials.
206 For this analysis, spontaneous activity was based on the intertrial interval (ITI).

207 *Influence of attention on thalamic Bursts:* Spiking activity in the thalamus is often segregated
208 into tonic and burst firing (Sherman, 2001). In tonic firing, thalamic neurons respond to
209 excitatory stimuli in a linear, constant fashion where the mean firing rate is proportional to the
210 strength of the stimulus. When thalamic neurons are sufficiently hyperpolarized to deinactivate

211 T-type Ca^{++} channels, they begin to exhibit bursting activity (McCormick and Huguenard, 1992).
212 As has been done previously (Reinagel et al., 1999; Alitto et al., 2019; Sanchez et al., 2023), we
213 tracked burst and tonic firing based on the following criteria: (1) an ISI of >100 ms that preceded
214 the first spike in a sequence, and (2) one or more subsequent spikes that followed with ISIs of
215 <4 ms. Past studies applying these criteria to intracellular recordings show that events defined
216 as bursts co-occur with T-channel plateau potentials (Lu et al., 1992). Based on these criteria,
217 we estimated the modulation of thalamic burst firing in the LGN by spatial attention.

218 *Modulation of response reliability by spatial attention:* To quantify the influence of spatial
219 attention on response reliability in the LGN, we calculated the Fano factor for both attend-toward
220 and attend-away trials (custom Matlab function). Fano factor is a common measure of response
221 reliability and is defined as:

222 $$Fano\ factor = \frac{spike\ count\ variance}{spike\ count\ mean}$$

223 *Support vector machine:* To quantify the influence of spatial attention at the population level, we
224 trained linear support vector machine (svm) classifiers using MATLAB's fitcsvm function on
225 pseudo-populations of sequentially recorded LGN neurons (Hastie et al., 2009). Pseudo-
226 populations were constructed using two strategies: with and without cell identity, both
227 incorporating bootstrap sampling over 10,000 iterations.

228 In the with cell identity condition, we constructed pseudo-population trials by randomly
229 sampling (with replacement) 20 attend-toward and 20 attend-away trials from each neuron. This
230 resulted in feature vectors with 198 features (one per neuron) and 40 trials per bootstrap
231 iteration. In the without cell identity condition, we generated feature vectors of the same size
232 (198 features × 40 trials), but the firing rates were drawn randomly from the entire pool of trials,
233 independent of neuron identity—effectively destroying the mapping between neurons and
234 features.

In both approaches, the SVM was trained on the pseudo-population and tested on a separate, non-overlapping validation set constructed using the same sampling procedure. Classifier performance was quantified using MATLAB's predict and perfcurve functions, with performance defined as the area under the curve (auc, receiver operator characteristic) on the validation data. To establish a chance-level baseline, we implemented a shuffle control in which trial labels (attend-toward vs. attend-away) were randomized prior to validation. Shuffled-label decoding was performed using the same bootstrap framework. Statistical comparison between real and shuffled models was based on the proportion of bootstrap iterations in which the real-model AUC exceeded the shuffled AUC.

To assess the distribution of attentional modulation across the LGN population, we implemented two additional SVM-based analyses: greedy ablation and reverse greedy ablation. In the greedy ablation analysis, we began with the full pseudo-population and iteratively removed the most informative neuron—defined as the neuron with the largest absolute SVM weight (beta coefficient). In the reverse greedy ablation analysis, we removed the least informative neuron at each step. In both cases, the classifier was retrained and evaluated after each ablation step using the same procedure described above.

Statistical tests: When testing for statistical differences between two populations, we performed bootstrap analyses to estimate median values, median difference values, 95% confidence intervals, and statistical significance. For this process, data were resampled with replacement 10,000 times while maintaining the original sample size in each resampling iteration. Within the text, statistics will be presented as:

median [95% confidence intervals]

for example:

toward trial F_1: 23.45 [19.23 - 29.85]

Where applicable, a bootstrap median difference estimation (BDE) is also provided. Throughout the Results, the distributions from bootstrap analyses are illustrated within the figures (e.g., Figure 1D-F). These histograms show the distribution of median values (or median difference values) generated from the 10,000 resamples with replacement. These distributions provide graphical estimates of effect size, variability, and statistical confidence. For within-neuron statistical tests, trials were shuffled across attention conditions (e.g., attend toward vs. attend away) and resampled with replacement 10,000 times per neuron. Statistical significance for each neuron was determined as the proportion of resampled values exceeding the observed effect size:

$$p = \frac{\sum_{i=1}^{10000} abs(median(resample_i)) \geq abs(observed)}{10000}$$

For sample-level statistical tests involving index values (e.g., attention index, burst index), significance was defined as the proportion of resampled values having the different sign as the observed value. Specifically, for an observed attention index >0, significance was calculated as:

$$p = \frac{\sum_{i=1}^{10000} median(resample_i) < 0}{10000}$$

For an observed attention index <0, significance was calculated as:

$$p = \frac{\sum_{i=1}^{10000} median(resample_i) > 0}{10000}$$

Results

To study the influence of attention on visual processing in the lateral geniculate nucleus (LGN), we trained two macaque monkeys (M1 and M2) to perform a spatial attention task (Figure 1A-B, see Materials and Methods). Briefly, the animals were trained to fixate on a colored dot while two drifting sinusoidal gratings, each surrounded by a thin colored circle, were shown in the periphery (mean eccentricity = 7.7°±3.3°, std). The contrast of the drifting gratings was held constant for a randomized interval (0.6s – 2.0s), at which point one of the gratings increased in contrast and the animal was rewarded for making a saccade to that location. The probability of each grating changing contrast was linked to the color of the fixation point. If the color of the fixation point matched the color of the surrounding circle, then that grating changed contrast on 90% of the trials (valid trials). On the remaining 10% of trials, the nonmatching grating changed contrast (invalid trials). Importantly, the color of the circles did not change from trial to trial; instead, the color of the fixation point changed. As expected, both monkeys were faster and more accurate on valid trials relative to invalid trials, indicating the animals were using covert spatial attention to perform the task (Figure 1 C-F; response latency: $valid_{M1}$ = 354ms [347 - 365], $invalid_{M1}$ = 390ms [361 - 405], BDE_{M1} = -34ms [-54 - -5], p_{M1} = 0.0094; $valid_{M2}$ = 301ms [298 - 303], $invalid_{M2}$ = 396ms [378 - 417], BDE_{M2} = -96ms [-117 - -77], $p_{M2} < 10^{-5}$); hit rate: $valid_{M1}$ = 0.949 [0.932 - 0.964], $invalid_{M1}$ = 0.749 [0.701 - 0.796], BDE_{M1} = 0.20 [0.152 - 0.249], $p_{M1} < 10^{-5}$; $valid_{M2}$ = 0.982 [0.979 - 0.985], $invalid_{M2}$ = 0.719 [0.672 - 0.767], BDE_{M2} = 0.263 [0.217 - 0.311], $p < 10^{-5}$).

To quantify the influence of spatial attention on the spiking activity of LGN neurons, we recorded the responses of 283 isolated single units (Figure 2, 103 magnocellular neurons, 180 parvocellular neurons; 151 off-cells, 132 on-cells) across both monkeys while they performed the spatial attention task. For each neuron, one of the drifting gratings was centered over the neuron's receptive field and the other grating was shown at an equidistant location from the

302 fixation point. Gratings were approximately 2-3 times the estimated size of the recorded
303 neuron's classical receptive field (typically 2° in diameter). Across cells and illustrated with the
304 examples shown in Figure 2, LGN responses to the drifting sine wave grating largely matched
305 the drift frequency of the grating (5 Hz). Thus, as is standard, we primarily focused on this
306 component (first harmonic, F_1) of the firing rate as quantified through Fourier analysis (see
307 Materials and Methods).

308 **Influence of spatial attention on neuronal firing rate**

309 Across our sample of LGN neurons, there was a small, but significant, increase in the F_1 of the
310 firing rate when the monkey directed attention toward the LGN cell's receptive field (toward
311 trials) relative to when it directed attention away from the receptive field (away trials) (Figure 3).
312 This effect was seen in M1 (Figure 3A-B (red data), toward = 26.1 [23.9 - 28.4] spikes/s, away =
313 25.2 [22.9 - 27.5] spikes/s, n = 161, BDE = 0.93 [0.56 - 1.32] spike/s, $p < 10^{-5}$) and M2 (Figure
314 3A-B (blue data), toward = 25.8 [23.1 - 28.4] spikes/s, away = 24.9 [22.255 - 27.476], n = 122,
315 BDE = 0.48 [0.10 - 0.92] spikes/s, p = 0.0059). This effect was also seen when data were
316 divided based on cell type (Figure 3C,D (parvocellular, red data), toward = 24.5 [22.8 – 26.2]
317 spikes/s, away = 23.9 [22.2 – 25.7] spikes/s, BDE = 0.54 [0.24 – 0.84] spike/s, p = 0.0001;
318 (magnocellular, blue data), toward = 29.1 [26.1 – 32.1] spikes/s, away = 28.0 [25.0 – 31.0], BDE
319 = 1.1 [0.57 – 1.67] spikes/s, $p < 10^{-5}$) and luminance polarity (Figure E-F, (off-center, black data)
320 toward = 26.9 [24.7 – 29.2] spikes/s, away = 26.2 [24.0 – 28.5], BDE = 0.72 [0.31 – 1.17]
321 spikes/s, $p < 10^{-5}$; (on-center, red data), toward = 25.2 [23.0 – 27.4] spikes/s, away = 24.5 [22.4
322 – 26.7] spikes/s, BDE = 0.76 [0.43 - 1.1] spikes/s, $p < 10^{-5}$). The differences between
323 parvocellular vs magnocellular (BDE = -0.16 [-0.73 – 0.33] spike/s, p = 0.31) and on-center vs
324 off-center (BDE = 0.12 [-0.36 – 0.60] spikes/s, p = 0.65) were not statistically significant. Similar
325 differences were seen for the mean response (F_0; data not shown), for M1 (toward = 27.4 [24.9 -
326 30.0] spikes/sec, away = 26.5 [24.0 - 29.0] spikes/sec, BDE = 0.92 [0.54 - 1.32] spikes/s, $p < 10^{-}$

^{5}) and M2 (toward = 30.6 [27.7 - 33.4] spikes/s, away = 30.0 [27.2 - 32.9] spikes/s, BDE = 0.54 [0.06 - 1.08] spikes/s, $p < 0.0114$). Across monkeys and cell types, the influence of attention on firing rate was significant, but small, increasing firing rate by ~ 1 spike/s.

Given that the firing rate varies from cell to cell, a bounded index is often useful for making comparisons between conditions across a sample of cells. We therefore used an attention index based on each cell's F_1 response, where

$$attention\ index = \frac{FR_{toward} - FR_{away}}{FR_{toward} + FR_{away}}$$

With the attention index, positive values indicate the firing rate increased with attention directed towards the neuron's receptive field and negative values indicate the firing rate decreased with attention. For both monkeys, median attention index values were significantly greater than zero (Figure 4A, D-E; M1: 0.014 [0.011 - 0.022], $p < 10^{-5}$; M2: 0.01 [0.001 - 0.012], $p = 0.0009$). When data was combined across monkeys an increased attention index was evident for parvocellular neurons (Figure 4F-G, 0.011 [0.003 - 0.015], $p = 0.0004$, $n = 180$), magnocellular neurons (Figure 4F-G, 0.012 [0.009 - 0.020], $p < 10^{-5}$, $n = 103$), on-cells (Figure 4H-I, 0.012 [0.007 - 0.018], $p < 10^{-5}$, $n = 131$), and off-cells (Figure 4H-I, 0.012 [0.004 - 0.015], $p < 10^{-5}$, $n = 152$). The differences between parvocellular and magnocellular neurons (parvocellular – magnocellular: -0.002 [-0.012 - 0.004], $p = 0.22$) as well as between on-center and off-center neurons (on-center – off-center: 0.001 [-0.006 - 0.009], $p = 0.41$) were not statistically significant. On a cell-by-cell basis, 16.6% of cells (47/283) had a statistically significant attention index at a significance level of 0.05 (Figure 4B). This distribution of statistically significant cells was marginally biased (Figure 4C, $p = 0.0479$) toward significantly positive attention index values (11.1% of cells) compared to significantly negative attention values (5.3% of cells). For the remainder of the paper, no statistically significant differences were seen between on-center and off-center data. Thus, on-center vs off-center differences will not be discussed.

351 Given that the influence of attention on firing rates appeared to be relatively small, we
352 wished to put this change into perspective and estimate its functional relevance. Since spatial
353 attention is often viewed as effectively increasing the contrast of the visual stimuli at that
354 attended location, we wanted to determine the change in stimulus contrast that would evoke the
355 same change in firing rate as shifting spatial attention toward the LGN receptive field (Figure 5).
356 We therefore calculated the attention equivalent contrast change (AECC, see Materials and
357 Methods). In the current study, the baseline contrast was set to be at the neuron's C50 (the
358 contrast that evoked a half-maximum response), but since each neuron's C50 was estimated
359 online with hand-mapping procedures, we used data from a separate population of neurons to
360 generate standardized contrast response functions for magnocellular (n = 33) and parvocellular
361 (n = 87) neurons (Figure 5A). Using these standardized functions, we calculated the contrast,
362 relative to the C50, that evoked the same change in firing rate as shifting spatial attention. For
363 example, if the change in firing rate caused by shifting attention was equivalent to the change in
364 firing rate caused by increasing the contrast from 30% to 40%, then the AECC would be 0.33.
365 For the parvocellular neurons in this study (Figure 5B-D), the 0.52 [0.097 - 0.785] spikes/s
366 increase in firing when spatial attention was shifted toward the cell's receptive field is equivalent
367 to a relative increase in contrast of only 0.025 [0.017 - 0.032] that is a change equal to 2.5% of
368 the C50. For a typical parvocellular neuron, this would be the equivalent of changing the
369 contrast from 50.0% to 51.25%. For magnocellular neurons (Figure 5B-D), the 0.681 [0.294 -
370 1.112] spikes/s increase in firing rate with attention is equivalent to a relative increase in
371 contrast of 0.058 [0.041 - 0.076]. For a typical C50 seen in magnocellular neurons, this would
372 be the equivalent of changing the contrast from 18.0 to 19.0. Across cells, equivalent contrast
373 change values were significantly greater for magnocellular neurons than for parvocellular
374 neurons (magno - parvo: 0.033 [0.014 - 0.052] p = 0.0002); however, for both cell types the
375 equivalent contrast change values were very small and likely would be below threshold for
376 change detection.

A separate metric that can be applied to assess the influence of spatial attention on visual responses utilizes receiver operating characteristic (ROC) analysis (Figure 6). With ROC analysis, one can ask how well an ideal observer would be able to determine, on a cell-by-cell basis, where the monkey was focusing its attention based solely on the response distributions (see Materials and Methods). A small difference in mean response would be discernable if there was also little variability (e.g., all trials with attention towards the cell's RF had the same small difference in firing rate compared to all away trials). At the opposite extreme, the same small difference in mean response would not be discernable if associated with much greater variability. In the first case with low variance, the ideal observer would successfully distinguish attend-towards and attend-away trials a high percent of the time. In the second case, the ideal observer would do much worse. Applying this approach, results indicate an ideal observer would have no difficulty discriminating either toward or away trial contrast changes from the baseline contrast (Figure 6A-B, D-I, toward = 0.912 [0.898 - 0.925], $p < 10^{-5}$; away = 0.902 [0.888 - 0.916], $p < 10^{-5}$). On a cell-by-cell basis, 97.2% of cells had a statistically significant toward trial vs baseline AUC and 96.5% of cells had a statistically significant away trial vs baseline AUC ($p<0.05$). However, and more importantly, the same methodology revealed that toward and away trials could only be discriminated with an accuracy of 0.522 (Figure 6C, 0.522 [0.513 - 0.532]). On a cell-by-cell basis, only 13.8% of cells had statistically significant toward vs away AUC ($p<0.05$). However, it is worth nothing that significant AUCs were more common ($p = 0.01$) for cells with greater activity while attending toward the LGN RF (n = 28, 9.9% of cells) compared to cells with greater activity while attending away from the LGN RF (n = 11, 3.9% of cells). Overall, these results indicate the influence of spatial attention in the LGN is weak and not a reliable indicator of where the animal was attending on a trial-to-trial basis.

Spatial attention and thalamic bursts

401 Across thalamic nuclei, relay cells produce spikes that can be categorized as burst spikes or
402 tonic spikes (Sherman, 2001). Although burst spikes are less common in alert animals
403 compared to anesthetized animals (Glenn and Steriade, 1982; Ramcharan et al., 2000; Alitto et
404 al., 2011), spatial attention could serve to modulate the relative occurrence of burst and tonic
405 spikes. Consistent with previous studies, results from this study show that burst spikes were
406 infrequent in the alert animal (Figure 7A). This was the case for trials when animals were
407 directed to attend towards the recorded cells' receptive fields (proportion burst spikes: all cells =
408 0.017 [0.015 - 0.018], M1 = 0.018 [0.016 - 0.021]; M2 = 0.014 [0.011 - 0.017], parvocellular cells
409 = 0.018 [0.015 - 0.020], magnocellular cells = 0.016 [0.013 - 0.019]) and away from the
410 recorded cells' receptive fields (proportion burst spikes: all cells = 0.016 [0.015 - 0.018]; M1 =
411 0.018 [0.016 - 0.021]; M2 = 0.015 [0.012 - 0.017], parvocellular cells = 0.017 [0.015 - 0.020];
412 magnocellular cells = 0.016 [0.013 - 0.019]). Further, shifts in spatial attention did not
413 significantly modulate the probability of an LGN neuron firing in burst mode as assessed using a
414 burst index:

415 $$burst\ index = \frac{(BP_{toward} - BP_{away}}{(BP_{toward} + BP_{away})}$$

416 (Figure 7B-D; burst index: M1 = 0.027 [-0.034 - 0.0088], p = 0.27; M2 = -0.004 [-0.074 - 0.061],
417 p = 0.44; parvocellular cells = -0.017 [-0.072 - 0.029], p = 0.35; magnocellular cells = -0.009 [-
418 0.088 - 0.009], p = 0.32). On a cell-by-cell basis, 11.7% of cells (33/283) had significant burst
419 index values, evenly split between more bursts during attend-toward trials (5.6%) and more
420 bursts during attend-away trials (6.0%) at a significance level of 0.05. There was, however, a
421 significant negative correlation between the firing rate of recorded cells and burst percent for
422 both toward trials (Figure 7E,F; r = -0.15 [-0.247 - -0.055], p = 0.001) and away trials (r = -0.17 [-
423 0.259 - -0.070], p = 0.0005). This inverse relationship might be explained by the time-voltage
424 relationship that governs the production of bursts which, in turn, may reflect variable levels of

425 alertness across/within recording sessions. Importantly, there was no correlation between burst
426 rate and the magnitude of spatial attention effects on the firing rate of LGN cells (r = 0.03 [-
427 0.150 - 0.091], p = 0.31).

428 **Influence of spatial attention on response reliability**

429 Past studies have shown that spatial attention increases response reliability in visual cortex
430 (Mitchell et al., 2007); however, this effect has not been previously demonstrated in the LGN. To
431 examine the influence of spatial attention on LGN response reliability, we calculated the Fano
432 factor (Fano factor = spike count variance / spike count mean) when animals were directed to
433 attend towards and away from the recorded neurons' receptive fields (Figure 8). Consistent with
434 results from studies not examining attention (Kara et al., 2000; Alitto et al., 2011), Fano factors
435 across our sample of LGN neurons were, on average, below 1.0, indicating the responses of
436 LGN neurons are less variable than expected from a Poisson process. This was the case for
437 trials when animals were cued to attend towards the recorded cells' receptive fields (Figure 8A,
438 Fano factor: M1 = 0.928 [0.908 - 0.958]; M2 = 0.924 [0.897 - 0.951], parvocellular cells = 0.932
439 [0.900 - 0.955]; magnocellular cells = 0.922 [0.908 - 0.968]; and away from the recorded cells'
440 receptive fields (Fano factor: M1 = 0.92 [0.91 - 0.94], M2 = 0.95 [0.90 - 0.98], parvocellular cells
441 = 0.932 [0.900 - 0.955]; magnocellular cells = 0.922 [0.908 - 0.968]). Although Fano factors
442 were extremely similar for attend towards and attend away trials, there was a significant
443 decrease in the Fano factor (as assessed using a Fano factor index, see Materials and
444 Methods) when attention was directed towards the receptive fields of recorded neurons (Figure
445 8B-D); FF Index: M1 = -0.005 [-0.010 - 0.000], p = 0.0306; M2 = -0.008 [-0.013 - -0.003], p =
446 0.0003; parvocellular cells = -0.004 [-0.008 - 0.000], p= 0.036; magnocellular cells = -0.010 [-
447 0.016 - -0.004], p = 0.0005). On a cell-by-cell basis 21.9% of cells had statistically significant
448 Fano factor index values (62/283), at a significant level of 0.05, with a significant bias (p =
449 0.0002) toward more cells with significantly negative FF index values (18%, more reliable during

450 attend-toward trials) compared cells with significantly positive FF index values (4.6%, more
451 reliable during attend away trials). Thus, similar to the effects of attention on firing rate, there
452 was a small, but significant, influence of attention on the response reliability of LGN neurons.

453 **Linear classification of LGN population activity**

454 Although the influence of spatial attention on visual responses in the LGN is statistically
455 significant, we have provided several lines of evidence that suggest the influence is unreliable,
456 weak, and unlikely to have a strong impact on downstream visual processing. However, our
457 core analyses treat each LGN recording independently and do not consider whether a more
458 reliable signal emerges at the population level. Ideally, this question would be addressed using
459 large numbers of simultaneously recorded LGN neurons. Unfortunately, our dataset consists of
460 many sequentially recorded single units, which limits our ability to study true population
461 dynamics.

462 Nevertheless, by constructing pseudo-populations from our data, we can ask whether
463 the attentional signal becomes more robust when LGN neurons are considered collectively.
464 Specifically, we asked whether an ideal observer (e.g., downstream neurons in V1) could
465 decode the attentional state of a given trial based on LGN population activity. To address this,
466 we used a linear classifier (support vector machine, svm) to test whether trials could be reliably
467 separated into attend-toward and attend-away categories based on pseudo-population activity
468 patterns. Each pseudo-population was constructed by randomly sampling (with replacement) 20
469 attend-toward trials and 20 attend-away trials from each neuron, resulting in 198 features
470 (neurons) and 40 samples (trials). The svm was trained on this dataset and tested on a
471 separate, non-overlapping validation set constructed in the same way.

472 Across 10,000 bootstrap iterations, the classifier achieved a mean classification
473 accuracy of ~75% (Figure 9A; auc = 0.754 +/- 0.001), which was significantly better different

474 than the label-shuffled control (auc = 0.499 +/- 0.001; p = 0.0164). The linear classifier
475 performed worse when only parvocellular data (Figure 9B; auc = 0.634 +/- 0.001, shuffle auc =
476 0.500 +/- 0.001, p = 0.1520) or magnocellular data (Figure 9C; auc = 0.659 +/- 0.001, shuffle
477 auc = 0.500 +/- 0.001, p = 0.1064) were used. This indicates that attentional modulation was not
478 confined to either the parvocellular or magnocellular pathways, consistent with our single-cell
479 analyses described above. Although both subpopulations performed worse than the full
480 population, this was likely due to the reduced number of neurons in these models; a size-
481 matched control population (containing both parvocellular and magnocellular neurons) also
482 performed worse than the full model (data not shown; AUC = 0.642 ± 0.001). Thus, the pseudo-
483 population analysis suggests that some attentional information is indeed present at the
484 population level in the LGN. We next asked whether this weak signal is broadly distributed
485 across the LGN population or carried by a small subset of neurons. To address this, we first
486 performed a "pooled" SVM analysis in which cell identity was erased. Pseudo-populations were
487 generated as before, but the firing rate values for each feature were randomly drawn from the
488 full pool of trials, independent of which neuron they came from. If the attentional signal was
489 distributed across many neurons, this pooling procedure should have preserved classifier
490 performance. However, it did not; the pooled model performed near chance (Figure 9D; auc =
491 0.507 ± 0.001), no better than the shuffled control (auc = 0.501 ± 0.001; p = 0.4772). This was
492 also the case when only parvocellular data (Figure 9E; auc = 0.506 +/- 0.001, shuffle auc =
493 0.500 +/- 0.001, p = 0.4786) or magnocellular data (Figure 9F; auc = 0.503 +/- 0.001, shuffle
494 auc = 0.500 +/- 0.001, p = 0.4897) were used. This suggests that the attentional signal is
495 concentrated in a minority of LGN neurons.

496 To further test this idea, we applied a "greedy ablation" svm analysis. Here, we began
497 with the full dataset and iteratively removed the most informative neuron, defined as the one
498 with the largest absolute valued beta coefficient, with retraining and re-evaluating the svm after

each step. Classifier performance rapidly declined toward chance after the removal of only ~10% of the neurons (Figure 10A–C), supporting the conclusion that only a small subset of neurons carries the attentional signal. The neurons removed from the model to reach chance discrimination performance were proportionally balanced between the parvocellular and magnocellular pathways compared to random draws from the underlying populations (parvocellular ablations = 14/191, magnocellular ablations = 6/70, $p = 0.8155$).

Conversely, we also performed a “reverse-greedy ablation” analysis, in which the least informative neurons were progressively removed. In this case, classifier performance improved as uninformative neurons were removed, peaking at auc = 0.859 ± 0.001 when ~18% of the neurons remained (Figure 10D–F). Together, these three complementary approaches strongly suggest that while an attentional signal is present in the LGN, it is not broadly distributed and is instead carried by a minority (~10–20%) of the neuronal population.

Discussion

It is generally agreed that the central nervous system lacks the resources to process all visual information that falls on the retina. Instead, the processing of behaviorally relevant information is prioritized at the expense of other, less- or non-relevant visual information. Spatial attention, the preferential processing of visual stimuli at a specific spatial location, is one mechanism that has a profound influence on what sensory information enters conscious perception. While early studies reported moderate attentional modulation in the lateral geniculate nucleus (LGN)—including increased BOLD signal in humans and enhanced parvocellular/magnocellular firing rates in primates (O'Connor et al., 2002; McAlonan et al., 2008) —subsequent findings have indicated otherwise (Jiang et al., 2015; Shah et al., 2022). Notably, Shah et al. (2022) did not find effects of attention in the LGN, despite observing strong attentional modulation in V1. Interestingly, while measures of spatial attention on visual processing within the LGN have been inconsistent using electrophysiology in non-human primates, the effect has been consistently observed in humans using BOLD fMRI analyses (Schneider and Kastner, 2009; Schneider, 2011; Ling et al., 2015; Poltoratski et al., 2019). Possible reasons for these differences are discussed below.

While the results reported here confirm that spatial attention does influence LGN activity (Figures 2 and 6), a deeper analysis of the data indicates that these effects are weak and inconsistent (Figures 3-5 and 9-10). The observed firing rate increases (on average, ~1 spike/s) corresponded to only a 1–1.8% contrast change, and ROC analysis showed that an ideal observer could barely distinguish attend-toward from attend-away trials (*53% accuracy*). Furthermore, burst firing, a key indicator of thalamic network state, remained unchanged. Finally, using support vector machine analysis of pseudo-populations constructed from our sequentially recorded LGN neurons, we found that attentional modulation was detectable in the population response patterns. However, this signal was limited to a small subset of LGN

538 neurons and did not generalize across the entire sample. Together, these findings suggest that
539 while spatial attention exerts a statistically significant influence on LGN processing, its functional
540 impact is weak.

541 Given its position between the retina and cortex (Usrey and Alitto, 2015), the LGN might
542 seem like an ideal site for attentional gating. Its small receptive fields could, in theory, support a
543 highly retinotopically precise spotlight of attention, which becomes harder to achieve in higher-
544 order cortex where receptive fields are larger. However, this is not how the visual system
545 operates. Instead, attentional modulation is strongest in higher-order areas (e.g., IT, MT)
546 (Connor et al., 1997; Seidemann and Newsome, 1999; Treue and Maunsell, 1999;
547 Ramezanpour and Fallah, 2022) and weakest at the early stages of processing (Luck et al.,
548 1997; Shah et al., 2022).

549 One possible reason is that early visual areas serve as a preprocessing hub,
550 establishing a basis set for the encoding of natural images that is robust against changes in
551 basic stimulus properties such as luminance and contrast (Shapley and Victor, 1979; Heeger,
552 1992; Olshausen and Field, 1996; Alitto and Usrey, 2004; Bonin et al., 2005; Priebe and
553 Ferster, 2012). When visual information reaches the cortex, V1 acts as a distribution hub
554 sending visual information down a variety of parallel pathways, each of which builds upon the
555 relatively simple, spatially compact receptive fields found in the early visual system, ultimately
556 resulting in a unified perception of the visual world (Felleman and Van Essen, 1991). Strong
557 attentional modulation at the LGN stage might introduce undesirable, nonspecific filtering,
558 affecting all downstream visual pathways indiscriminately. A more efficient strategy is to reserve
559 strong attentional modulation for higher-order areas where receptive fields are already task-
560 tuned, for example, MT during motion discrimination or FFA during face recognition. Thus, in the
561 context of spatial attention, the role of the LGN is to maintain a stable, unbiased flow of retinal

562 input to V1, where visual information is distributed across parallel processing streams before
563 attentional filtering occurs at later stages.

564 A parallel can be drawn to arousal-driven LGN modulation, which globally enhances or
565 suppresses visual signals depending on behavioral state (Molnár et al., 2021; Crombie et al.,
566 2024). Unlike spatial attention, arousal-based modulation affects all LGN neurons
567 indiscriminately, ensuring coordinated gain control rather than interfering with specific spatial
568 and/or feature-processing streams. Similarly, LGN activity is suppressed during modality-
569 specific attention to non-visual tasks, a scenario where broad suppression is beneficial rather
570 than disruptive (Wimmer et al., 2015).

571 Animal and human experimental models often provide complementary evidence that,
572 when combined, help build a more complete understanding of brain function. In the case of
573 spatial attention and neural processing in the LGN, the two models appear to provide unique
574 insight into how attention affects different components of the neural circuitry. In humans, spatial
575 attention has been reliably shown to modulate LGN activity as measured by BOLD fMRI
576 (Schneider and Kastner, 2009; Schneider, 2011; Ling et al., 2015; Poltoratski et al., 2019). In
577 contrast, similar experiments in nonhuman primates using extracellular recordings to measure
578 spiking activity have yielded far more variable results, ranging from relatively robust modulation
579 to none at all (McAlonan et al., 2008; Jiang et al., 2015; Shah et al., 2022).

580 The reasons for this discrepancy are unclear, but a key methodological difference lies in
581 the fundamental unit of measurement accessible to each technique. The BOLD signal reflects
582 changes in blood oxygenation and is sensitive to the activity of large neural populations—
583 potentially hundreds of thousands of neurons within a single voxel—averaged over both space
584 and time, which should improve the detection of small changes in firing rate. Importantly, while
585 the BOLD signal is influenced by both spiking and subthreshold synaptic activity, it is only
586 weakly correlated with the spiking output of the underlying network. Thus, it should be viewed

587 as primarily reflecting aggregate input and local processing (Logothetis et al., 2001; Logothetis,
588 2008).

589 In contrast, extracellular electrophysiology captures the spiking activity of individual
590 neurons, is largely blind to subthreshold events, and provides a direct readout of the output of
591 the local network to downstream targets. Traditional single-unit recordings, including those used
592 in the present study, typically capture only one or two neurons at a time. Even with modern
593 multi-electrode arrays, the number of neurons recorded simultaneously is orders of magnitude
594 smaller than the population contributing to a single fMRI voxel. Thus, while fMRI provides a
595 population-level view of neural dynamics emphasizing pre-synaptic activity, extracellular
596 recordings offer a highly resolved but sparse sampling of network output. This fundamental
597 difference in spatial scale and sensitivity likely contributes to the apparent inconsistency in
598 results across methodologies.

599 One potential path toward resolving this discrepancy is to apply analytical methods that
600 characterize population dynamics rather than focusing solely on individual neuron activity. Such
601 an approach, applied to a sufficiently large sample of LGN neurons, may more reliably reveal an
602 underlying influence of spatial attention on LGN processing. Although the current data set is not
603 ideal for this type of analysis (e.g., neurons were not recorded simultaneously), we took steps in
604 this direction by applying support vector machine (svm) classification to our sequentially
605 recorded data. Overall, this analysis partially supports the view that a population code enriches
606 the detectability of spatial attention in the LGN; however, the influence of spatial attention is not
607 evenly distributed across our recording sample. Instead, the svm models suggest that
608 attentional modulation in the LGN is carried by ~10-20% of the neurons in our sample. This is in
609 line with our finding that 16.6% of LGN neurons had a statistically significant attention index. Of
610 course, this conclusion does not account for possible temporal dynamics in population activity
611 which could depend on how attention influences a variety of factors including network state

612 dynamics (van Kempen et al., 2021; Shi et al., 2022) and noise correlations (Cohen and
613 Maunsell, 2009; Ruff and Cohen, 2014)

614 If we are to conclude that only a small percentage of LGN neurons are modulated by
615 attention, there are at least three possible scenarios regarding this subpopulation. First, the
616 modulated neurons may correspond to a known LGN cell type, such as inhibitory interneurons
617 or misclassified koniocellular neurons. Second, the modulated neurons may represent a
618 previously unidentified functional subtype. Finally, it is possible that the modulated neurons do
619 not form a distinct category at all. Instead, the attentional signal may be weak, temporally
620 unstable, and only rarely sufficient to drive detectable changes in spiking activity of LGN
621 neurons.

622 Finally, we would like to address how the results of the SVM analysis should be
623 interpreted in the context of our data. While SVM classification can be informative, it may also
624 miss the functional point of LGN activity during spatial attention. An SVM asks whether an ideal
625 observer could accurately classify attentional state based on the joint activity of an n-
626 dimensional neuronal population (Pooresmaeili et al., 2010). Any neuron whose firing rate is
627 reliably modulated by attention—regardless of whether that modulation is an increase or a
628 decrease—can contribute to building a linear decision boundary in this space. In this sense,
629 both increases and decreases in firing rate are equally useful to the classifier (Hastie et al.,
630 2009).

631 While SVM classification is a valuable analytical tool, a literal interpretation of the results
632 can be misleading. LGN neurons do not "encode" attentional state, nor is there reason to
633 believe that downstream areas such as V1 are trying to "decode" attentional state based on
634 LGN spiking activity. The LGN's functional role is to relay visual information from the retina to
635 the cortex. Spatial attention, likely via non-retinal sources, modulates this relay by slightly
636 prioritizing the transmission of signals that originate from attended regions of visual space. In

637 this view, the attentional state is not encoded in the LGN per se but instead alters the gain or
638 fidelity of visual signals being passed through it.

639

640

641 ## Figure Legends

642 **Figure 1.** Spatial attention task and psychophysical measure of spatial attention. Two macaque
643 monkeys (Monkey 1: M1 and Monkey 2: M2) were trained to perform a covert spatial attention
644 task. ***A-B***. On each trial, animals maintained fixation on a central green dot while two peripheral
645 sine wave gratings appeared, each surrounded by a colored circle. One grating was positioned
646 over the receptive field of a recorded LGN neuron (dashed black circle) and the other at an
647 equidistant location. The color of the fixation point, in conjunction with the colors of the
648 peripheral circles, indicated the probability that each grating would undergo a contrast increase
649 after a brief delay. In 90% of trials (**A1, B1**), termed "valid trials", the contrast change occurred
650 at the location where the circle color matched the fixation cue. In 10% of trials (**A2, B2**), termed
651 invalid trials, the contrast change occurred at the non-matching location. Since one stimulus
652 was positioned inside the receptive field and one was positioned outside the receptive field,
653 trials were further categorized based on the spatial relationship between the cued location and
654 the RF. "Attend toward" trials **(A)** occurred when the cued stimulus was positioned inside the
655 receptive field, while "attend away" trials **(B**) occurred when the cued stimulus was positioned
656 away from the receptive field. The error bars in **C and B** indicate the 25th and 75th percentiles.
657 Animals were rewarded for making a saccade to the grating that increased in contrast. Both
658 animals respond faster (***C, D***) and more accurately (***E, F***) on valid trials compared to invalid
659 trials. Statistical significance was assessed using bootstrap difference estimation (BDE). Panels
660 D and F show the distribution of median differences (valid – invalid) computed over 10,000

bootstrap resamples for M1 (red) and M2 (blue). These distributions provide graphical estimates of effect size, variability, and statistical confidence (see Methods and Materials for details).

Figure 2. Single-unit examples of lateral geniculate nucleus (LGN) responses recorded while the animal performed the spatial attention task. Each row (***A - F***) shows data from one neuron. ***Column 1***. Peri-stimulus time histograms (PSTHs) showing firing rates for valid *attend-toward* (red) and *attend-away* (blue) trials, aligned to the time of contrast change (0 s). ***Column 2***. Mean firing rate across all trials as a function of time relative to the start of recording. ***Column 3***. Distribution of firing rates (F_1) across all trials. ***Column 4***. Cumulative distribution of firing rates across all trials. In all panels, the shaded areas indicate standard error of the mean.

Figure 3. Firing rate during spatial attention. ***A***. Distribution of firing rates (f1) for attend toward vs attend away trials across all cells (M1 = red, M2 = blue; n = 283). ***B***. Significance of these effects was determined via a bootstrap difference estimation (See Materials and Methods). The red and blue data in panel ***B*** show the distribution of median difference values (toward – away) over 10,000 resamples with replacement for M1 and M2, respectively. These distributions provide a direct graphical illustration of statistical significance and confidence intervals (p values in text). ***C, D***. Same as ***A, B*** for parvocellular (red) and magnocellular (blue) data. ***E, F***. Same as ***A, B*** for on-center (red) and off-center (black).

Figure 4. Attention index. ***A***. Distribution of attention index values across cell types (error bars = 25th and 75th percentiles). ***B***. Overall distribution of attention index values. Significant values ($p < 0.05$) are indicated in black. ***C***. Significance of the distribution of attention index values (positive > negative) was determined by a bootstrap null distribution analysis (red dashed line = observed difference). ***D***. Distribution of attention index values for M1 (red) and M2 (blue) (0 = black dashed line). ***E***. Significance of these distributions was determined via a bootstrap mean estimation. ***F, G***. Same as ***D, E*** for parvocellular (red) and magnocellular (blue) data. ***H, I***. Same as ***A, B*** for on-center (red) and off-center (black) data.

686 **Figure 5.** Equivalent contrast change. ***A***. Population contrast response functions for
687 parvocellular (red) and magnocellular (blue) data (shaded area = standard error of the mean).
688 ***B, C***. Distribution of equivalent contrast values across cell types (error bars = 25th and 75th
689 percentiles). ***D***. Significance of these distributions was determined via a bootstrap mean
690 estimation.

691 **Figure 6.** ROC analysis of spatial attention. ***A***. Area under the curve (AUC) for attend toward
692 trials vs baseline, across cell types. ***B***. Area under the curve for attend away trials vs baseline,
693 across cell types. ***C***. Area under the curve for attend toward trials vs attend away trials, across
694 cell types. ***D***. Distribution of AUC values for M1 (red = toward vs baseline, blue = away vs
695 baseline, black = toward vs away). ***E***. Same as ***D*** for M2. F. Same as ***D*** for parvocellular data.
696 ***G***. Same as ***D*** for magnocellular data.

697 **Figure 7.** Thalamic bursts during spatial attention. ***A***. Distribution of thalamic burst percentage
698 for attend toward trials vs attend away trials. ***B***. Sample distributions for burst index values
699 across cell types. ***C, D***. Significance of these effects illustrated via a bootstrap difference
700 estimation. ***E***. Correlation between burst percentage and firing rate across all cell types (red =
701 attend toward trials, blue = attend away trials, dashed line = linear fit). ***F.*** Significance of these
702 correlations illustrated via a bootstrap mean estimation.

703 **Figure 8.** Response reliability during spatial attention. ***A***. Distribution of Fano factor values for
704 attend toward trials vs attend away trials. ***B***. Sample distributions for Fano factor index values
705 across cell types. ***C, D***. Significance of these effects as illustrated via a bootstrap difference
706 estimation.

707 **Figure 9.** LGN population activity is weakly modulated by spatial attention. Support vector
708 machine (SVM) models were used to assess whether population-level activity in the LGN could
709 predict the subject's attentional state**. A.** Distributions of classification performance (area under

710 the curve, auc) for svm models trained on pseudo-populations that preserved cell identity (red),
711 compared to shuffled-label controls (blue). **B.** Same analysis as in A, but using "pooled" pseudo-
712 populations in which cell identity was randomized. The sharp drop in performance suggests that
713 the attentional signal is not broadly distributed across the population.

714 **Figure 10**. A minority of LGN neurons carry the attentional signal. SVM models were iteratively
715 ablated to assess the relative contribution of individual neurons to the population-level
716 attentional signal. **A.** "Greedy ablation" analysis: the most informative neurons were
717 progressively removed from the model. AUC is plotted as a function of ablation number (0 = full
718 dataset). Shaded areas show ±1 standard deviation across bootstrap iterations. **B.** AUC
719 distribution for the full model (198 neurons). **C.** AUC distribution after 20 greedy ablations,
720 demonstrating a drop to chance performance. **D.** "Reverse greedy ablation" analysis: the least
721 informative neurons were progressively removed. Classifier performance increased as
722 uninformative neurons were removed, peaking with ~18% of the neurons remaining. **E.** AUC
723 distribution for the full model. **F.** AUC distribution after 141 ablations, corresponding to peak
724 model performance.

725

726 ## References

727 Alitto H, Rathbun DL, Vandeleest JJ, Alexander PC, Usrey WM (2019) The augmentation of
728 retinogeniculate communication during thalamic burst mode. J Neurosci 39:5697–5710.

729 Alitto HJ, Moore BD, Rathbun DL, Usrey WM (2011) A comparison of visual responses in the
730 lateral geniculate nucleus of alert and anaesthetized macaque monkeys. J Physiol 589:87–
731 99.

732 Alitto HJ, Usrey WM (2004) Influence of contrast on orientation and temporal frequency tuning

733 in ferret primary visual cortex. J Neurophysiol 91:2797–808.

734 Baldwin MKL, Balaram P, Kaas JH (2017) The evolution and functions of nuclei of the visual
735 pulvinar in primates. J Comp Neurol 525:3207–3226.

736 Bonin V, Mante V, Carandini M (2005) The suppressive field of neurons in lateral geniculate
737 nucleus. J Neurosci 25:10844–10856.

738 Boshra R, Kastner S (2022) Attention control in the primate brain. Curr Opin Neurobiol
739 76:102605.

740 Carrasco M, Ling S, Read S (2004) Attention alters appearance. Nat Neurosci 7:308–313.

741 Cerkevich CM, Lyon DC, Balaram P, Kaas JH (2014) Distribution of cortical neurons projecting
742 to the superior colliculus in macaque monkeys. Eye Brain 23:121–137.

743 Cohen MR, Maunsell JHR (2009) Attention improves performance primarily by reducing
744 interneuronal correlations. Nat Neurosci 12:1594–1600.

745 Connor CE, Preddie DC, Gallant JL, Van Essen DC (1997) Spatial Attention Effects in Macaque
746 Area V4. J Neurosci 17:3201–3214.

747 Crombie D, Spacek MA, Leibold C, Busse L (2024) Spiking activity in the visual thalamus is
748 coupled to pupil dynamics across temporal scales. PLoS Biol 22:e3002614.

749 Felleman DJ, Van Essen DC (1991) Distributed hierarchical processing in the primate cerebral
750 cortex. Cereb Cortex 1:1–47.

751 Glenn LL, Steriade M (1982) Discharge rate and excitability of cortically projecting intralaminar
752 thalamic neurons during waking and sleep states. J Neurosci 2:1387–1404.

753 Hastie T, Tibshirani R, Friedman J (2009) The Elements of Statistical Learning, 2nd ed. New
754 York: Springer US.

755 Heeger DJ (1992) Normalization of cell responses in cat striate cortex. Vis Neurosci 9:181–197.

756 Jiang Y, Yampolsky D, Purushothaman G, Casagrande VA (2015) Perceptual decision related
757 activity in the lateral geniculate nucleus. J Neurophysiol 114:717–735.

758 Kara P, Reinagel P, Reid RC (2000) Low response variability in simultaneously recorded retinal,
759 thalamic, and cortical neurons. Neuron 27:635–646.

760 Kastner S, Ungerleider LG (2000) Mechanisms of visual attention in the human cortex. Annu
761 Rev Neurosci.

762 Lauritzen TZ, Ales JM, Wade AR (2010) The effects of visuospatial attention measured across
763 visual cortex using source-imaged, steady-state EEG. J Vis 10.

764 Ling S, Pratte MS, Tong F (2015) Attention alters orientation processing in the human lateral
765 geniculate nucleus. Nat Neurosci 18:496–498.

766 Logothetis NK (2008) What we can do and what we cannot do with fMRI. Nature 453:869–878.

767 Logothetis NK, Pauls J, Augath M, Trinath T, Oeltermann A (2001) Neurophysiological
768 investigation of the basis of the fMRI signal. Nature 412:150–157.

769 Lu SM, Guido W, Sherman SM (1992) Effects of membrane voltage on receptive field properties
770 of lateral geniculate neurons in the cat: Contributions of the low-threshold Ca2+
771 conductance. J Neurophysiol 68:2185–2198.

772 Luck SJ, Chelazzi L, Hillyard SA, Desimone R (1997) Neural mechanisms of spatial selective
773 attention in areas V1, V2, and V4 of macaque visual cortex. J Neurophysiol 77:24–42.

774 Lynch JC, Graybiel AM, Lobeck LJ (1985) The differential projection of two cytoarchitectonic
775 subregions of the inferior parietal lobule of macaque upon the deep layers of the superior
776 colliculus. J Comp Neurol 235:241–254.

Martinez-Trujillo J (2022) Visual Attention in the Prefrontal Cortex. Annu Rev Vis Sci 8:407–425.

Maunsell JHR (2015) Neuronal Mechanisms of Visual Attention. Annu Rev Vis Sci 1:373–391.

McAdams CJ, Reid RC (2005) Attention modulates the responses of simple cells in monkey primary visual cortex. J Neurosci 25:11023–11033.

McAlonan K, Cavanaugh J, Wurtz RH (2008) Guarding the gateway to cortex with attention in visual thalamus. Nature 456:391–394.

McCormick DA, Huguenard JR (1992) A model of the electrophysiological properties of thalamocortical relay neurons. J Neurophysiol 68:1384–1400.

McCormick DA, McGinley MJ, Salkoff DB (2015) Brain state dependent activity in the cortex and thalamus. Curr Opin Neurobiol 31:133–140.

Meyyappan S, Rajan A, Yang Q, Mangun GR, Ding M (2025) Decoding Visual Spatial Attention Control. eNeuro 12.

Mitchell JF, Sundberg KA, Reynolds JH (2009) Spatial Attention Decorrelates Intrinsic Activity Fluctuations in Macaque Area V4. Neuron 63:879–888.

Mitchell JF, Sundberg KA, Reynolds JH (2007) Differential attention-dependent response modulation across cell classes in macaque visual area V4. Neuron 55:131–141.

Molnár B, Sere P, Bordé S, Koós K, Zsigri N, Horváth P, Lőrincz ML (2021) Cell Type-Specific Arousal-Dependent Modulation of Thalamic Activity in the Lateral Geniculate Nucleus. Cereb cortex Commun 2:tgab020.

Ni AM, Maunsell JHR (2019) Neuronal Effects of Spatial and Feature Attention Differ Due to Normalization. J Neurosci 39:5493–5505.

O'Connor DH, Fukui MM, Pinsk MA, Kastner S (2002) Attention modulates responses in the

799 human lateral geniculate nucleus. Nat Neurosci 5:1203–1209.

800 Olshausen BA, Field DJ (1996) Emergence of simple-cell receptive field properties by learning a
801 sparse code for natural images. Nature 381:607–609.

802 Poltoratski S, Maier A, Newton AT, Tong F (2019) Figure-Ground Modulation in the Human
803 Lateral Geniculate Nucleus Is Distinguishable from Top-Down Attention. Curr Biol
804 29:2051-2057.e3.

805 Pooresmaeili A, Poort J, Thiele A, Roelfsema PR (2010) Separable codes for attention and
806 luminance contrast in the primary visual cortex. J Neurosci Off J Soc Neurosci 30:12701–
807 12711.

808 Posner MI (1980) Orienting of attention. Q J Exp Psychol 32:3–25.

809 Priebe NJ, Ferster D (2012) Mechanisms of neuronal computation in mammalian visual cortex.
810 Neuron 75:194–208.

811 Ramcharan EJ, Gnadt JW, Sherman SM (2000) Burst and tonic firing in thalamic cells of
812 unanesthetized, behaving monkeys. Vis Neurosci 17:55–62.

813 Ramezanpour H, Fallah M (2022) The role of temporal cortex in the control of attention. Curr
814 Res Neurobiol 3:100038.

815 Reinagel P, Godwin D, Sherman SM, Koch C (1999) Encoding of visual information by LGN
816 bursts. J Neurophysiol 81:2558–2569.

817 Reynolds JH, Chelazzi L (2004) Attentional modulation of visual processing. Annu Rev Neurosci
818 27:611–647.

819 Ruff DA, Cohen MR (2014) Attention can either increase or decrease spike count correlations in
820 visual cortex. Nat Neurosci 17:1591–1597.

821 Saalmann YB, Kastner S (2011) Cognitive and perceptual functions of the visual thalamus.
822 Neuron 71:209–223.

823 Sanchez AN, Alitto HJ, Rathbun DL, Fisher TG, Usrey WM (2023) Stimulus contrast modulates
824 burst activity in the lateral geniculate nucleus. Curr Res Neurobiol 4:100096.

825 Schneider KA (2011) Subcortical mechanisms of feature-based attention. J Neurosci Off J Soc
826 Neurosci 31:8643–8653.

827 Schneider KA, Kastner S (2009) Effects of sustained spatial attention in the human lateral
828 geniculate nucleus and superior colliculus. J Neurosci Off J Soc Neurosci 29:1784–1795.

829 Seidemann E, Newsome WT (1999) Effect of spatial attention on the responses of area MT
830 neurons. J Neurophysiol 81:1783–1794.

831 Shah S, Mancarella M, Hembrook-Short JR, Mock VL, Briggs F (2022) Attention differentially
832 modulates multiunit activity in the lateral geniculate nucleus and V1 of macaque monkeys.
833 J Comp Neurol 530:1064–1080.

834 Shapley RM, Victor JD (1979) Nonlinear spatial summation and the contrast gain control of cat
835 retinal ganglion cells. J Physiol 290:141–161.

836 Sherman SM (2001) Tonic and burst firing: dual modes of thalamocortical relay. Trends
837 Neurosci 24:122–126.

838 Sherman SM, Guillery RW (2002) The role of the thalamus in the flow of information to the
839 cortex. Philos Trans R Soc London Ser B, Biol Sci 357:1695–1708.

840 Sherman SM, Usrey WM (2021) Cortical control of behavior and attention from an evolutionary
841 perspective. Neuron 109:3048–3054.

842 Shi Y-L, Steinmetz NA, Moore T, Boahen K, Engel TA (2022) Cortical state dynamics and

843 selective attention define the spatial pattern of correlated variability in neocortex. Nat
844 Commun 13:44.

845 Treue S, Maunsell JH (1999) Effects of attention on the processing of motion in macaque
846 middle temporal and medial superior temporal visual cortical areas. J Neurosci Off J Soc
847 Neurosci 19:7591–7602.

848 Usrey WM, Alitto HJ (2015) Visual Functions of the Thalamus. Annu Rev Vis Sci 1:351–371.

849 van Kempen J, Gieselmann MA, Boyd M, Steinmetz NA, Moore T, Engel TA, Thiele A (2021)
850 Top-down coordination of local cortical state during selective attention. Neuron 109:894-
851 904.e8.

852 Wimmer RD, Schmitt LI, Davidson TJ, Nakajima M, Deisseroth K, Halassa MM (2015) Thalamic
853 control of sensory selection in divided attention. Nature 526:705–709.

854 Zénon A, Krauzlis RJ (2012) Attention deficits without cortical neuronal deficits. Nature
855 489:434–437.

856 Zhou H, Schafer RJ, Desimone R (2016) Pulvinar-Cortex interactions in vision and attention.
857 Neuron 89:209–220.

858

Figure 1

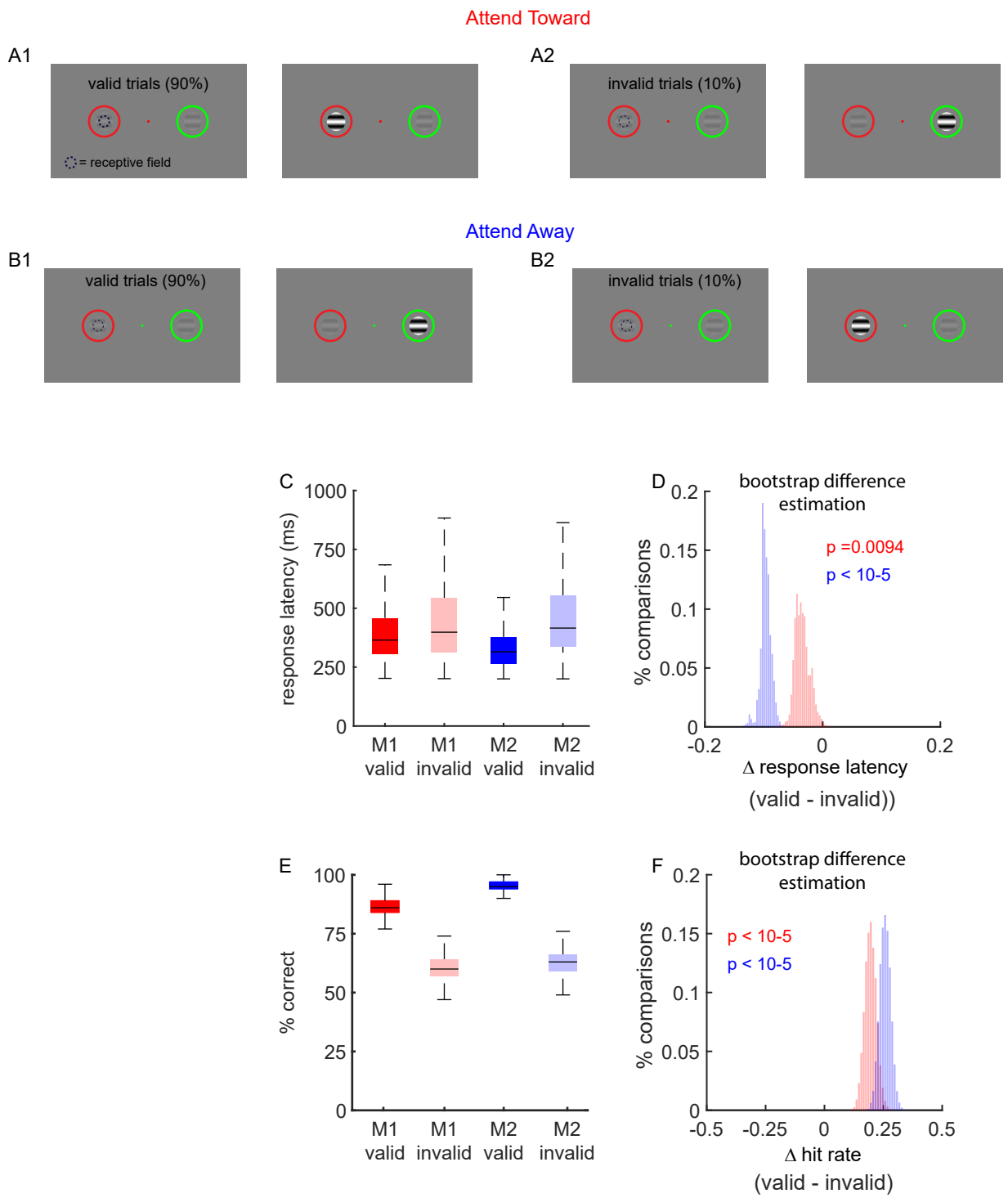
Attend Toward
A1
valid trials (90%)
= receptive field
A2
invalid trials (10%)
Attend Away
B1
valid trials (90%)
B2
invalid trials (10%)
C
response latency (ms)
1000
750
500
250
0
M1 valid
M1 invalid
M2 valid
M2 invalid
D
bootstrap difference estimation
p =0.0094
p < 10-5
% comparisons
0.2
0.15
0.1
0.05
0
-0.2
0
0.2
Δ response latency
(valid - invalid))
E
% correct
100
75
50
25
0
M1 valid
M1 invalid
M2 valid
M2 invalid
F
bootstrap difference estimation
p < 10-5
p < 10-5
% comparisons
0.2
0.15
0.1
0.05
0
-0.5
-0.25
0
0.25
0.5
Δ hit rate
(valid - invalid)

Figure 2

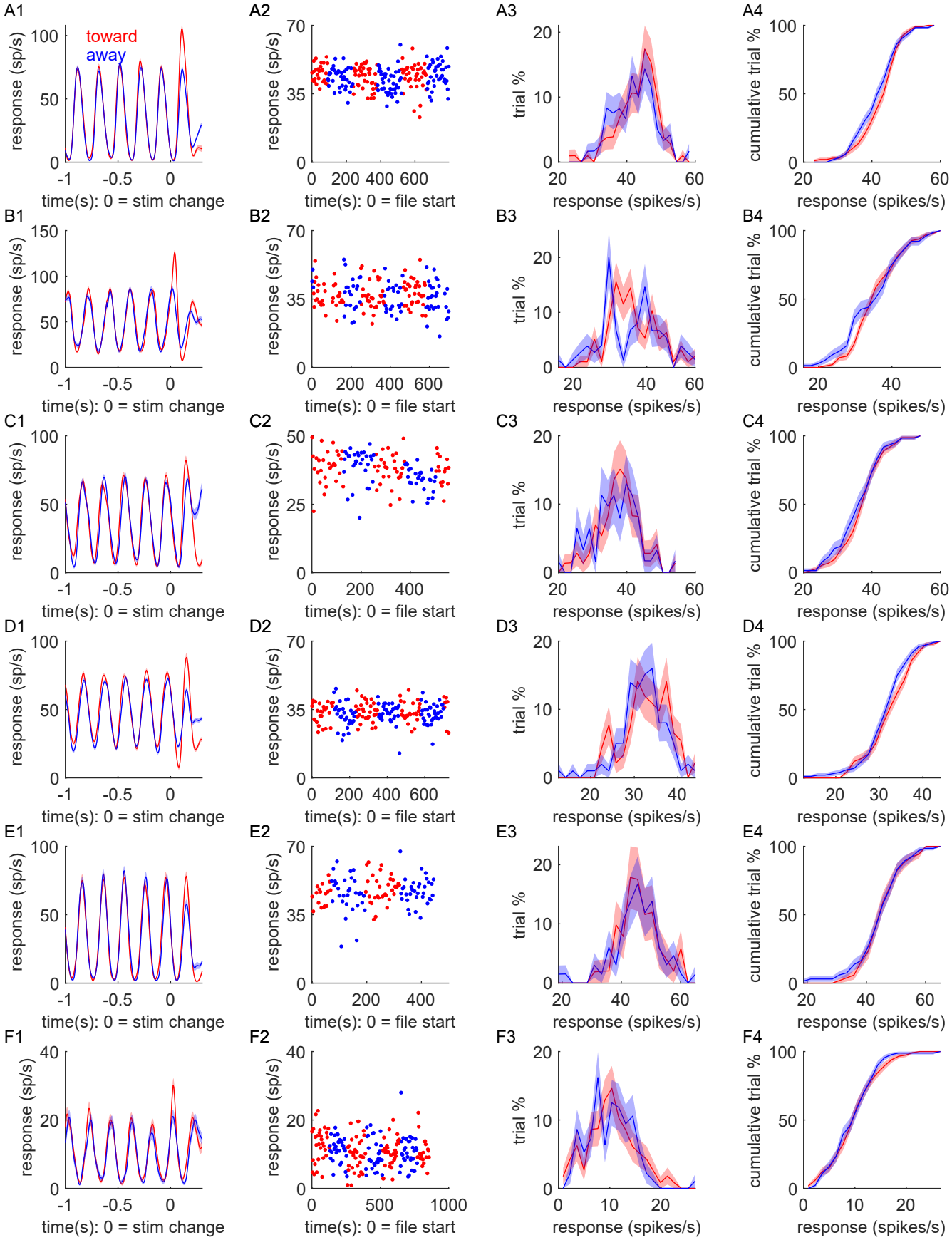
A1
A2
A3
A4
B1
B2
B3
B4
C1
C2
C3
C4
D1
D2
D3
D4
E1
E2
E3
E4
F1
F2
F3
F4
toward
away
response (sp/s)
time(s): 0 = stim change
time(s): 0 = file start
trial %
cumulative trial %
response (spikes/s)

Figure 3

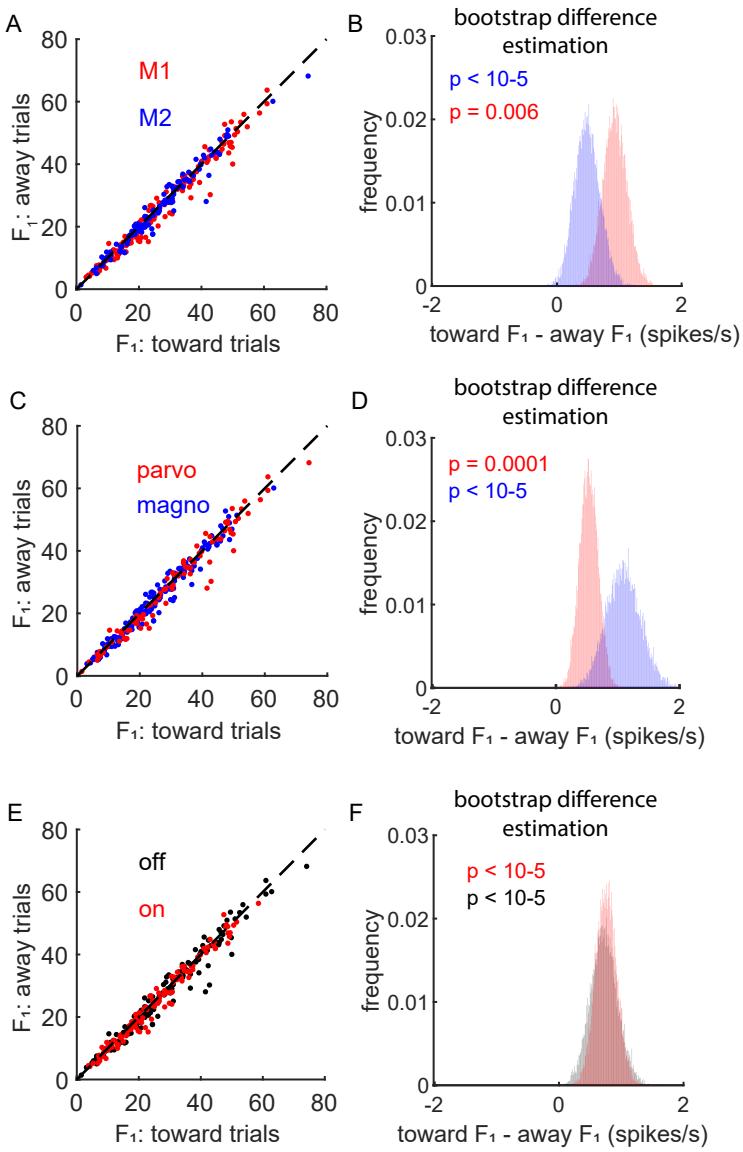
A
M1
M2
F1: away trials
F1: toward trials
B
bootstrap difference estimation
p < 10-5
p = 0.006
frequency
toward F1 - away F1 (spikes/s)
C
parvo
magno
F1: away trials
F1: toward trials
D
bootstrap difference estimation
p = 0.0001
p < 10-5
frequency
toward F1 - away F1 (spikes/s)
E
off
on
F1: away trials
F1: toward trials
F
bootstrap difference estimation
p < 10-5
p < 10-5
frequency
toward F1 - away F1 (spikes/s)

Figure 4

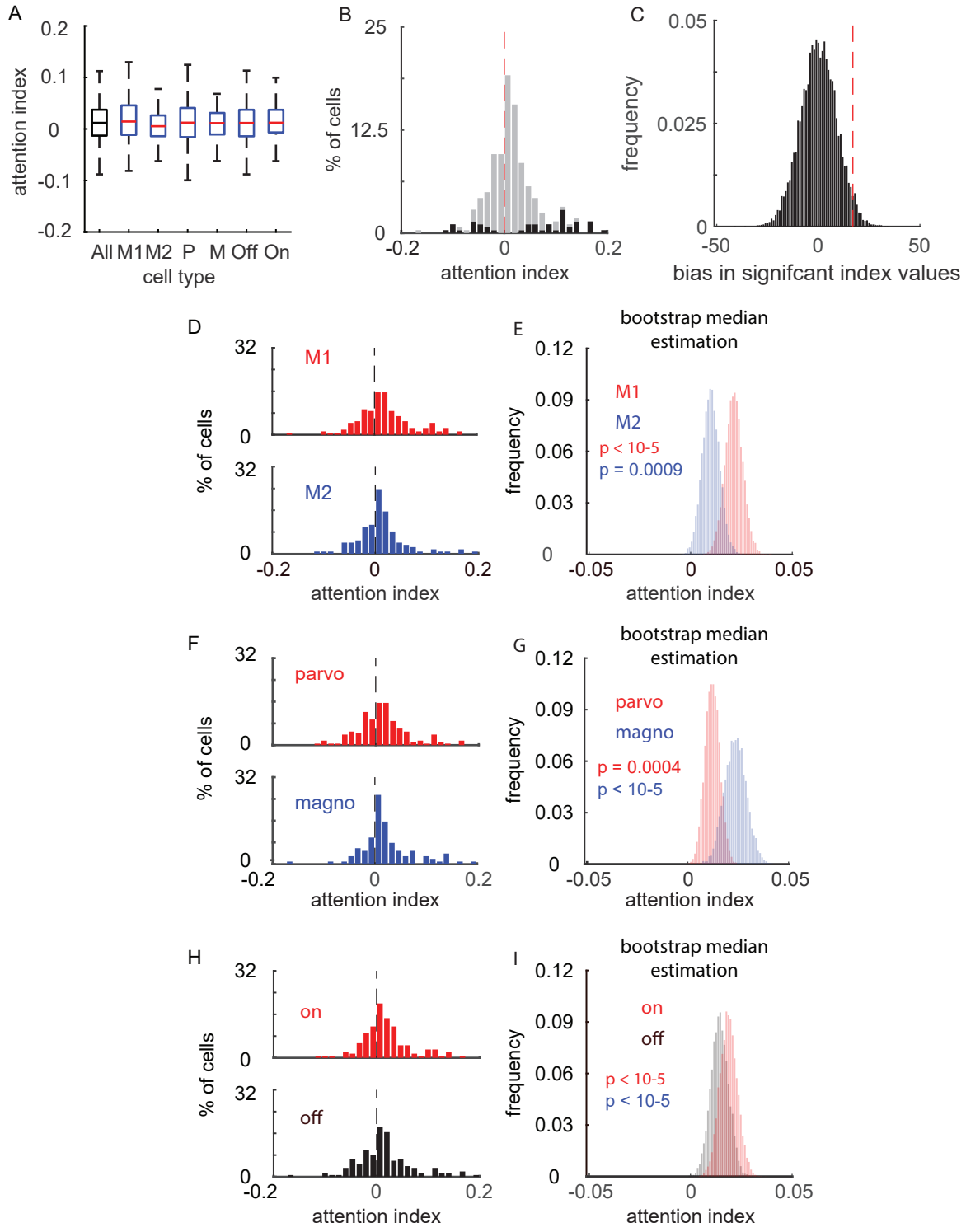
A
attention index
0.2
0.1
0
-0.1
-0.2
All M1 M2 P M Off On
cell type
B
% of cells
25
12.5
0
-0.2
0
0.2
attention index
C
frequency
0.05
0.025
0
-50
0
50
bias in signifcant index values
D
% of cells
32
M1
0
32
M2
0
-0.2
0
0.2
attention index
E
bootstrap median estimation
frequency
0.12
0.09
0.06
0.03
0
M1
M2
p < 10-5
p = 0.0009
-0.05
0
0.05
attention index
F
% of cells
32
parvo
0
32
magno
0
-0.2
0
0.2
attention index
G
bootstrap median estimation
frequency
0.12
0.09
0.06
0.03
0
parvo
magno
p = 0.0004
p < 10-5
-0.05
0
0.05
attention index
H
% of cells
32
on
0
32
off
0
-0.2
0
0.2
attention index
I
bootstrap median estimation
frequency
0.12
0.09
0.06
0.03
0
on
off
p < 10-5
p < 10-5
-0.05
0
0.05
attention index

Figure 5

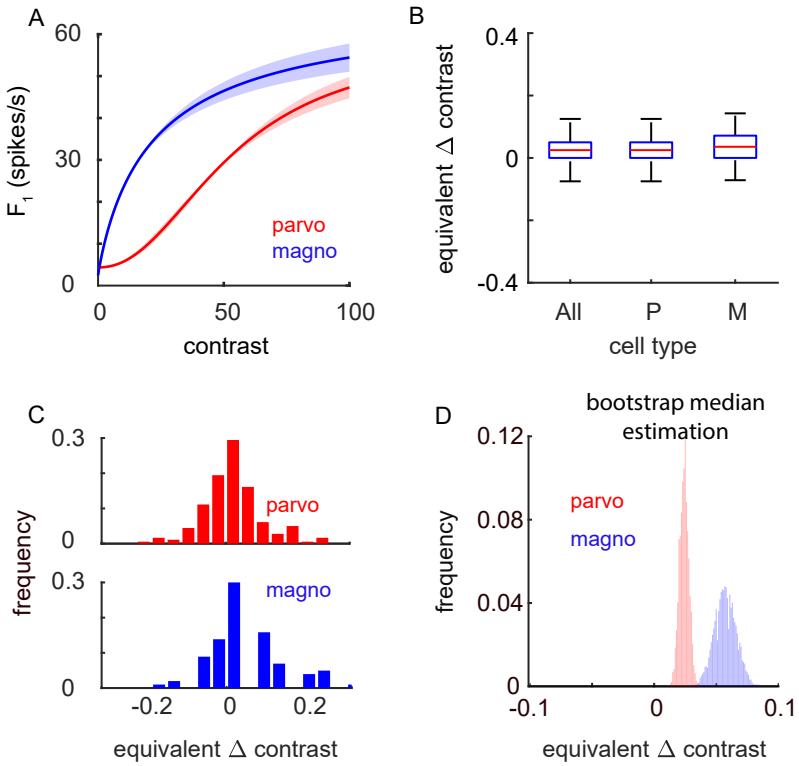
A
60
30
0
F_1 (spikes/s)
0
50
100
contrast
parvo
magno
B
0.4
0
-0.4
equivalent Δ contrast
All
P
M
cell type
C
0.3
0
frequency
parvo
0.3
0
magno
-0.2
0
0.2
equivalent Δ contrast
D
bootstrap median
estimation
0.12
0.08
0.04
0
frequency
parvo
magno
-0.1
0
0.1
equivalent Δ contrast

Figure 6

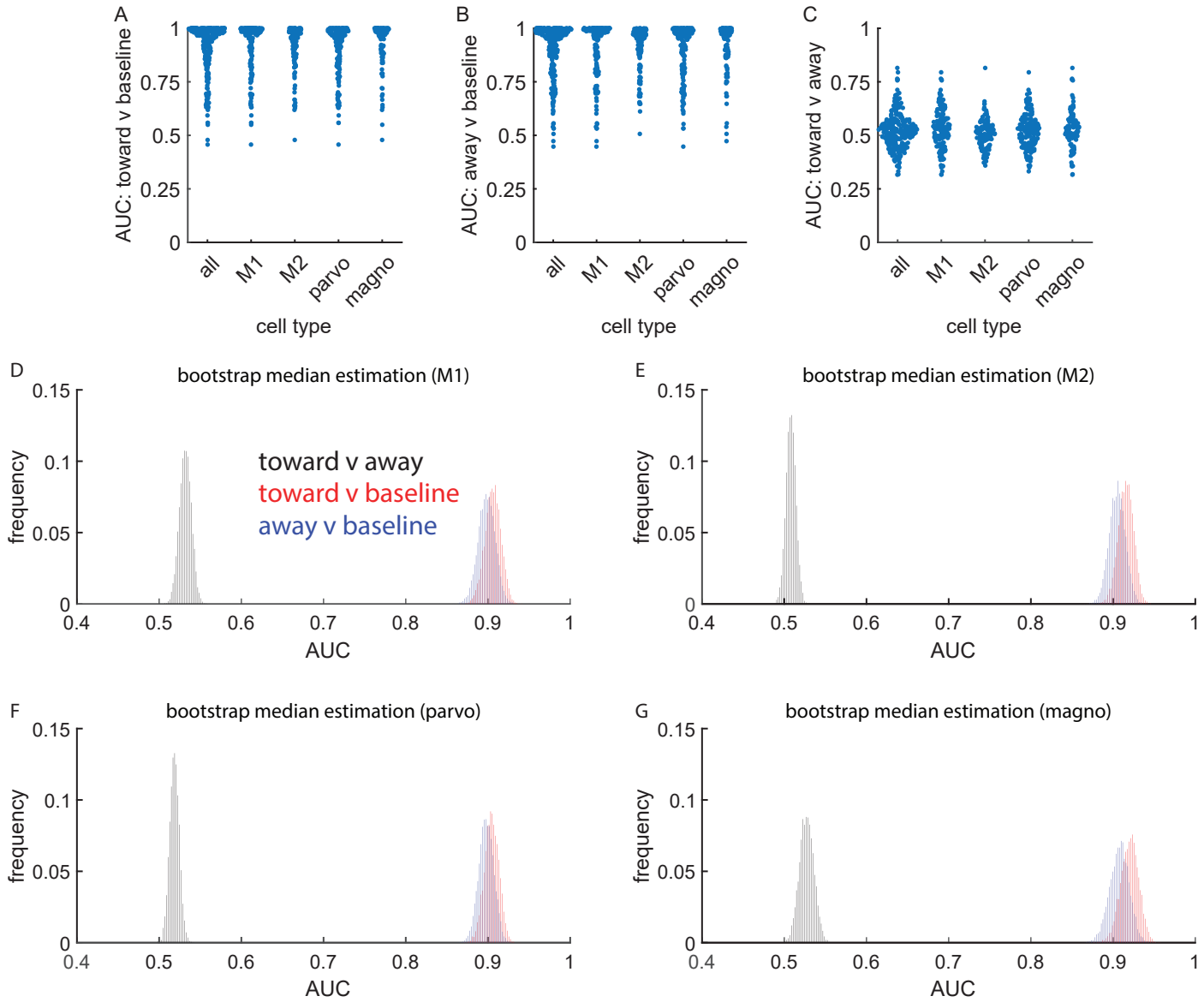
A
AUC: toward v baseline
1
0.75
0.5
0.25
0
all
M1
M2
parvo
magno
cell type
B
AUC: away v baseline
C
AUC: toward v away
D
bootstrap median estimation (M1)
frequency
0.15
0.1
0.05
toward v away
toward v baseline
away v baseline
0.4
0.5
0.6
0.7
0.8
0.9
AUC
E
bootstrap median estimation (M2)
F
bootstrap median estimation (parvo)
G
bootstrap median estimation (magno)

Figure 7

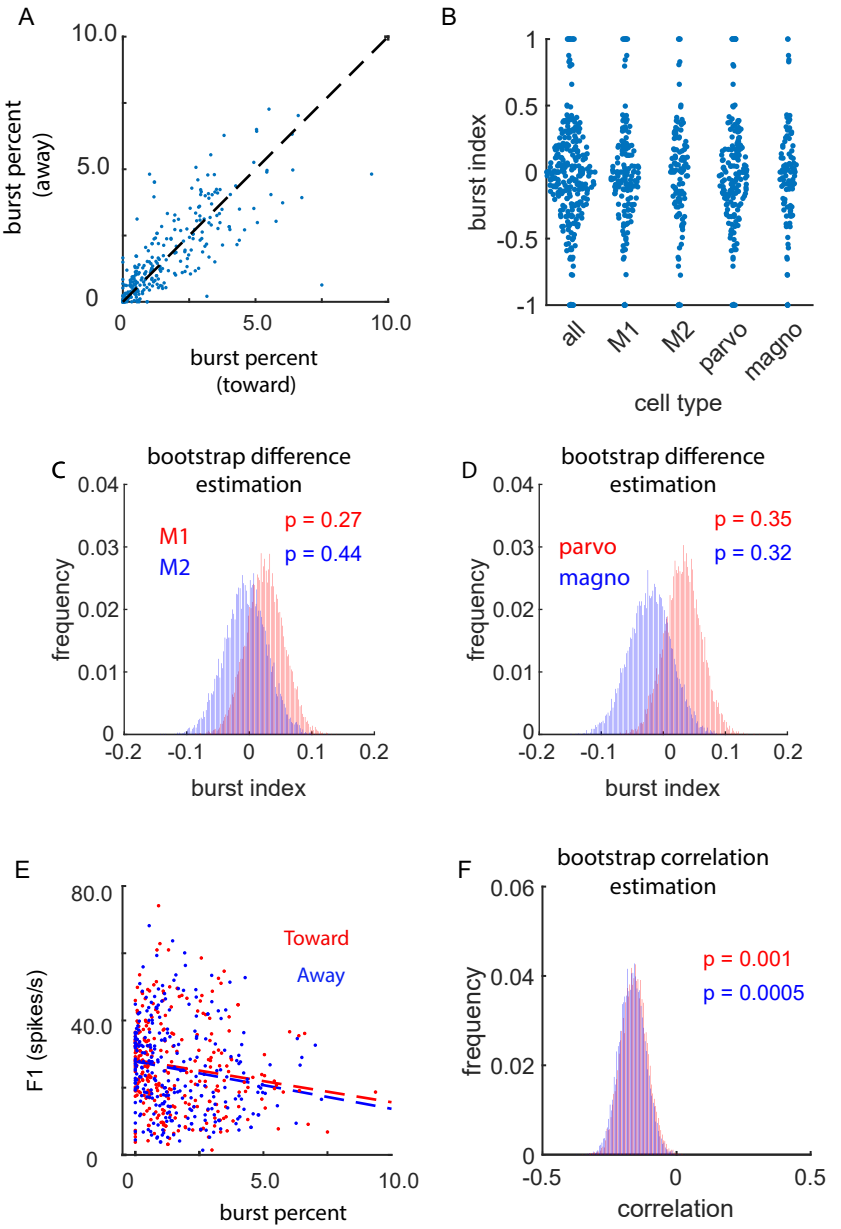
A
burst percent (away)
burst percent (toward)
B
burst index
all
M1
M2
parvo
magno
cell type
C
bootstrap difference estimation
M1
M2
p = 0.27
p = 0.44
frequency
burst index
D
bootstrap difference estimation
parvo
magno
p = 0.35
p = 0.32
frequency
burst index
E
F1 (spikes/s)
Toward
Away
burst percent
F
bootstrap correlation estimation
p = 0.001
p = 0.0005
frequency
correlation

Figure 8

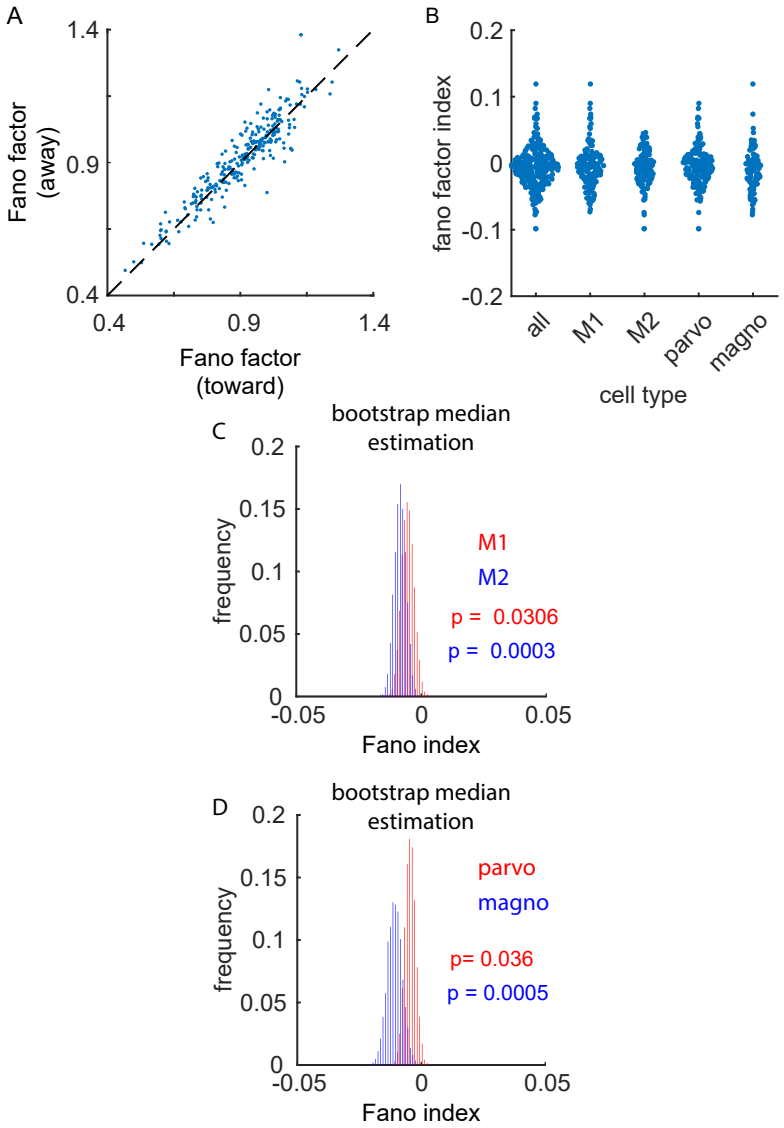
A
1.4
0.9
0.4
Fano factor (away)
0.4
0.9
1.4
Fano factor (toward)
B
0.2
0.1
0
-0.1
-0.2
fano factor index
all
M1
M2
parvo
magno
cell type
C
bootstrap median estimation
0.2
0.15
0.1
0.05
0
frequency
M1
M2
p = 0.0306
p = 0.0003
-0.05
0
0.05
Fano index
D
bootstrap median estimation
0.2
0.15
0.1
0.05
0
frequency
parvo
magno
p= 0.036
p = 0.0005
-0.05
0
0.05
Fano index

Figure 9

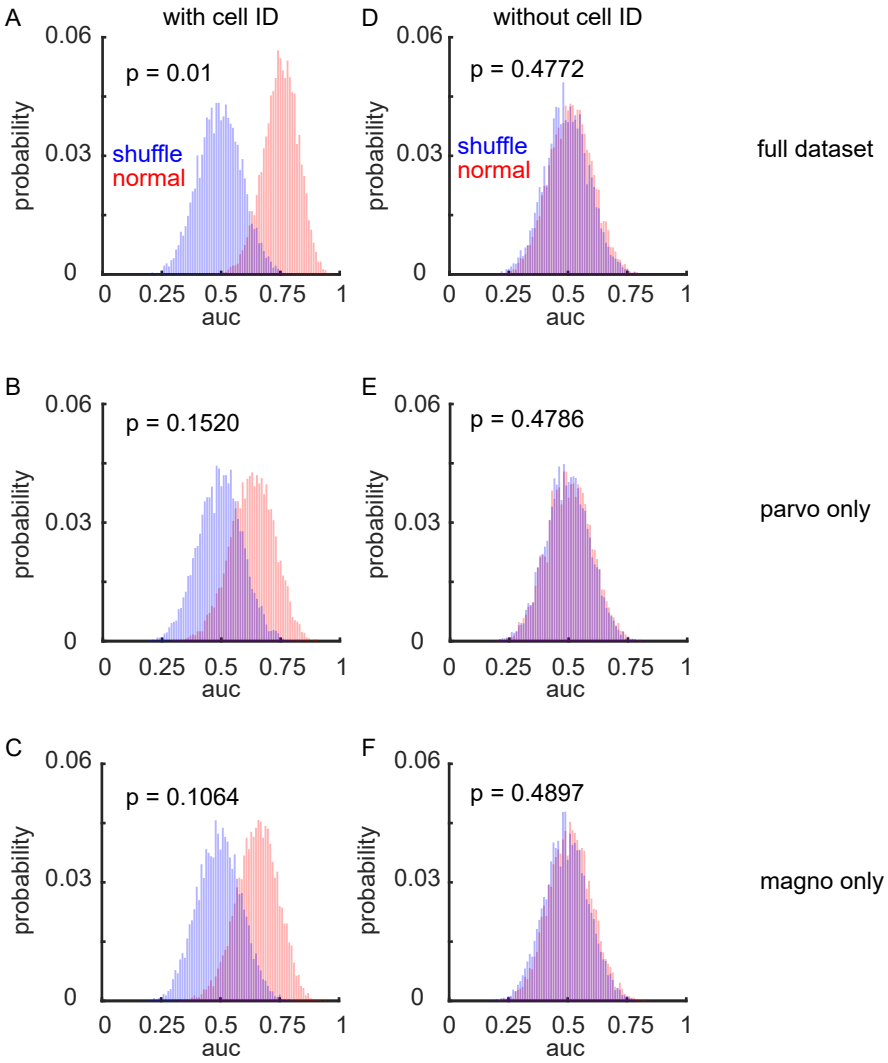
A
with cell ID
p = 0.01
shuffle
normal
probability
0.06
0.03
0
0 0.25 0.5 0.75 1
auc
D
without cell ID
p = 0.4772
shuffle
normal
probability
0.06
0.03
0
0 0.25 0.5 0.75 1
auc
full dataset
B
p = 0.1520
probability
0.06
0.03
0
0 0.25 0.5 0.75 1
auc
E
p = 0.4786
probability
0.06
0.03
0
0 0.25 0.5 0.75 1
auc
parvo only
C
p = 0.1064
probability
0.06
0.03
0
0 0.25 0.5 0.75 1
auc
F
p = 0.4897
probability
0.06
0.03
0
0 0.25 0.5 0.75 1
auc
magno only

Figure 10

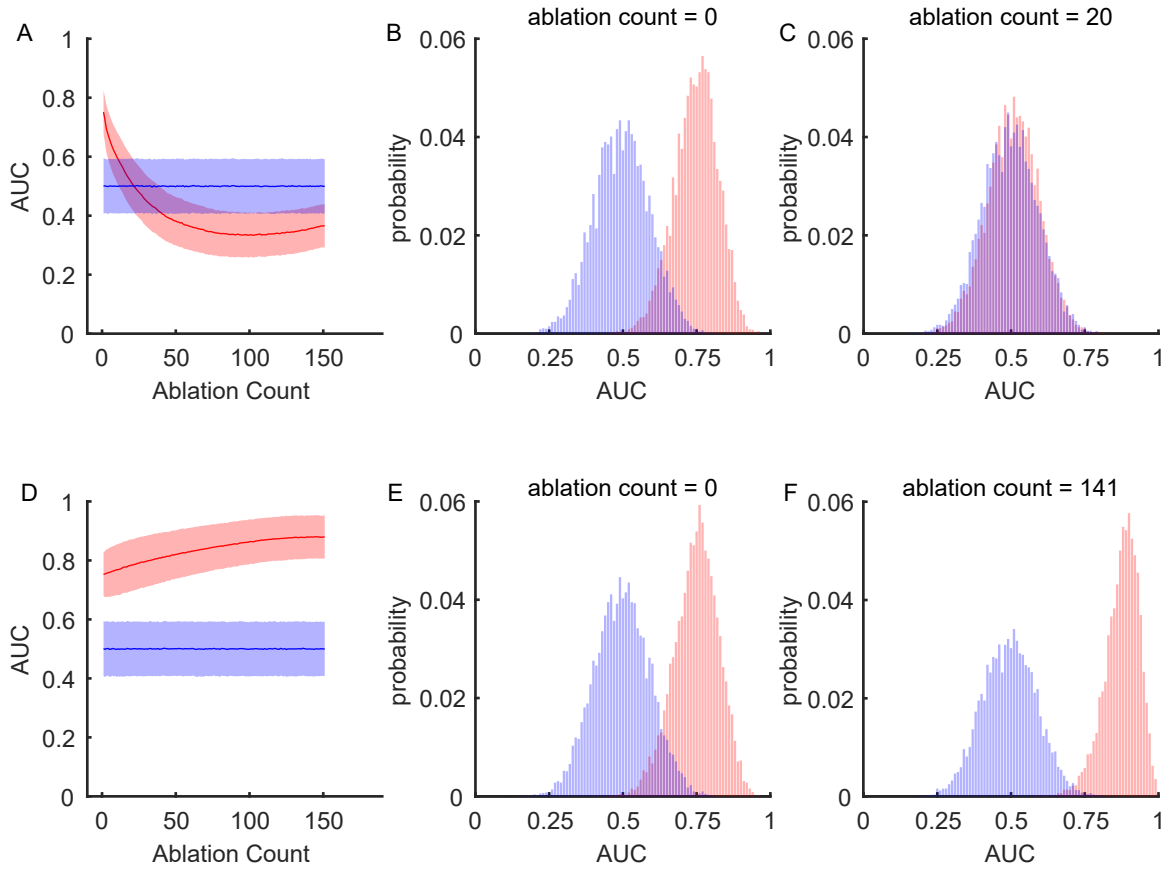
A
AUC
Ablation Count
B
ablation count = 0
probability
AUC
C
ablation count = 20
probability
AUC
D
AUC
Ablation Count
E
ablation count = 0
probability
AUC
F
ablation count = 141
probability
AUC